EFFECTS OF Mn DOPING ON THE OPTICAL PROPERTIES OF Zn_2GeO_4 PHOSPHOR PREPARED THROUGH CO-PRECIPITATION

N. M. C. Hoang Phuong Lan [1], C. X. Thang [1*], N. D. T. Kien [1*], V.-H. Pham [1], T. T. An [1], N. V. Tung [2]

[1] Advanced Institute for Science and Technology (AIST), Hanoi University of Science and Technology (HUST), Hanoi, Vietnam; e-mail: thang.caoxuan@hust.edu.vn
[2] Institute of Science and Technology, Ministry of Public Security, Hanoi, Vietnam

Zn_2GeO_4 (ZGO) phosphor and Mn-doped ZGO (ZGO:Mn^{2+}) phosphor were successfully synthesized through co-precipitation. Results indicated that Zn ions were successfully replaced by Mn ions, and Mn doping led to a lattice contraction. Under UV light excitation, the undoped ZGO exhibited a strong white-bluish emission at 517 nm and weak green emission at 530 nm, both of which were attributed to the native defects in the ZGO host. The near infrared emission (~740 nm) was attributed to the transfer of energy from non-bridging oxygen-hole centers to zinc (Zn_i) and oxygen-vacant state (Vo) in the ZGO host. ZGO:Mn^{2+} emitted a band at ~535 nm which originated from the $^4T_1$–$^6A_1$ transition of Mn^{2+} ion. These initial findings showed that the luminescence properties in the green and near infrared range of ZGO phosphor can be controlled.

Keywords: *luminescence, Zn_2GeO_4, co-precipitation, ZGO phosphor, ZGO:Mn^{2+}.*

ВЛИЯНИЕ ЛЕГИРОВАНИЯ МАРГАНЦЕМ НА ОПТИЧЕСКИЕ СВОЙСТВА ЛЮМИНОФОРА Zn_2GeO_4, ПОЛУЧЕННОГО МЕТОДОМ СООСАЖДЕНИЯ

N. M. C. Hoang Phuong Lan [1], C. X. Thang [1*], N. D. T. Kien [1*], V.-H. Pham [1], T. T. An [1], N. V. Tung [2]

УДК 535.37

[1] Передовой институт науки и технологий Ханойского университета науки и технологий, Ханой, Вьетнам; e-mail: thang.caoxuan@hust.edu.vn
[2] Институт науки и технологий Министерства общественной безопасности, Ханой, Вьетнам

(Поступила 17 марта 2020)

Методом соосаждения синтезированы люминофоры Zn_2GeO_4 (ZGO) и ZGO (ZGO:Mn^{2+}), легированный Mn. Установлено, что ионы Zn заменяются ионами Mn, а легирование Mn приводит к сжатию решетки. При возбуждении УФ-излучением нелегированный ZGO демонстрирует сильное бело-голубоватое свечение при 517 нм и слабое зеленое излучение при 530 нм. Обе полосы приписаны естественным дефектам в матрице ZGO. Эмиссия в ближнем ИК-диапазоне (~740 нм) объяснена переносом энергии от немостиковых кислородно-дырочных центров к цинку (Zn_i) и кислородно-вакантному состоянию (V_O) в матрице ZGO. ZGO:Mn^{2+} излучает полосу при ~535 нм, которая появляется в результате перехода $^4T_1$–$^6A_1$ иона Mn^{2+}. Показано, что люминесцентными свойствами в зеленом и ближнем ИК-диапазоне люминофора ZGO можно управлять.

Ключевые слова: *люминесценция, Zn_2GeO_4, соосаждение, люминофор ZGO, ZGO:Mn^{2+}.*

Introduction. Zinc orthogermanate (ZGO) is a phosphor with white–bluish luminescence and a wide band gap of 4.68 eV and could emit an integrated luminescent intensity 40% higher than commercial ZnO phosphors [1]. In the last 10 years, ZGO materials have been of interest for their optical and thermal features. Although many papers on ZGO have been published, their optical properties are still of special interest because they can be changed mainly through fabrication and ion doping. Under the excitation of UV and near

UV light, the ZGO phosphor emits a broadband from blue to red color. Under manganese doping (ZGO:Mn^{2+}), the Mn^{2+} ions replace the Zn^{2+} ions of the host lattice, and a green emission spectrum is emitted from the transition $^4T_1$–$^6A_1$ of the Mn^{2+} ions [2]. Many works have focused on ZGO:Mn^{2+} materials for the application of this green emission in biomedicine and phosphor for LED and FED screens [3–5]. Different synthesis methods, such as solid phase reaction, sol-gel, and solvothermal reaction, have been used to produce undoped and Mn^{2+}-doped ZGO. To the best of the authors' knowledge, no research has focused on ZGO:Mn^{2+} materials synthesized through co-precipitation.

The undoped and Mn-doped ZGO phosphor were synthesized through co-precipitation. Different structural characterization techniques such as X-ray diffraction (RD), field emission scanning electron microscopy (FESEM), and energy-dispersive X-ray spectroscopy (EDS), were used to verify whether Mn^{2+} ions replace Zn^{2+} ions in the host lattice. UV-vis and PL were applied to investigate the effect of synthesis condition on the optical properties of ZGO. The energy transfer mechanism in ZGO host lattice was also proposed.

Experiment. Undoped and Mn^{2+}-doped ZGO were synthesized via co-precipitation using GeO_2 powders (99.99% Sigma–Aldrich), $Zn(CH_3COO)_2 \cdot 2H_2O$ (≥98% purity, Aldrich), NaOH (≥97 % purity, Sigma–Aldrich), and $Mn(NO_3)_2$ (99.9% purity, Aldrich) as precursor materials. For the synthesis of Mn^{2+}-doped ZGO, the ratio between $Mn(NO_3)_2$ and other precursors to dope ZGO with 5 mol.% Mn^{2+} concentration was calculated.

The synthesis process was as follows: 1 mmol GeO_2 and 2 mmol NaOH were added into 10 mL of deionized water. Mixing ends were conducted after completely dissolving the GeO_2 powder. The second solution containing 2 mmol $Zn(CH_3COO)_2 \cdot 2H_2O$, and 20 mL of deionized water was prepared. The third solution is a mixture of 0.05 mmol $Mn(NO_3)_2$ and 10 mL of deionized water. All these solutions were mixed and stirred together to form a homogeneous solution for precipitation. The as-obtained precipitate was then filtered, centrifuged, and washed several times using deionized water (DI) water and ethanol. The powders were then dried at 80°C for 24 h in a vacuum drying oven. Finally, all the samples were calcined in a furnace with temperature set in the range from 800 to 1200°C.

The crystal structures of ZGO and ZGO:0.05Mn^{2+} were analyzed by X-ray diffraction (XRD, D8 Advance, Bruker, Germany) with CuK_α radiation (λ = 1.5418 Å) and 2θ =10–70°. The morphologies of the samples were studied by field emission scanning electron microscopy (JEOL, JSM 6700F, JEOL Techniques, Tokyo, Japan) and an energy dispersive spectroscopy (EDS) to examine optical properties and chemical composition. Photoluminescence (PL) measurements using a NANO LOG spectrofluorometer (Horiba, USA) equipped with 450 W Xe arc lamp and double excitation monochromators were performed to evaluate the optical properties of the Mn-doped ZGO. All samples were investigated with a PMS-80 UV-VIS NEAR IR spectra analysis system of ZGO and ZGO:Mn^{2+} phosphor.

Results and discussion. The influence of calcinating temperature on the formation of ZGO samples was investigated. Figure 1 shows the typical XRD patterns of the samples prepared with different calcinating temperatures ranging from 800 to 1200°C. For the samples calcinated at 800, 900, 1000, and 1100°C, diffraction peaks corresponding to the rhombohedral Zn_2GeO_4 phase (JCPDS No.11-0687) and the GeO_2 phase (JCPDS No.36-1463) were observed. In addition to the synthesized Zn_2GeO_4 phase, the GeO_2 phase was found and can be attributed to the by-product $Ge(OH)_4$ that was reversely transformed into GeO_2 through calcination at high temperatures.

When the as-synthesized powder was calcinated at 1200°C, diffraction peaks corresponding to ZGO were observed in the XRD pattern, indicating that the sample was pure ZGO. Given that the melting temperature of GeO_2 is approximately 1115°C, the purity of the sample can be explained as follows. During the calcination at 1200°C, the by-product $Ge(OH)_4$ was reversely transformed to GeO_2, which then was melted and incorporated to form homogeneous ZGO crystals.

On the basis of the X-ray diffraction results of the ZGO host lattice, the calcining temperature for ZGO:Mn^{2+} was selected at 1200°C. Figure 2a shows the XRD patterns of undoped ZGO host and 5 mol% Mn^{2+}-doped ZGO that were both calcinated at 1200°C. All the diffraction peaks of the samples can be assigned to a pure rhombohedral ZGO phase (JCPDS No. 110687). No extra peak was observed in the XRD patterns from the undoped and Mn^{2+}-doped ZGO, suggesting that the Mn^{2+} ions were completely replaced in the ZGO lattice. A zoom-in of the XRD patterns with 2θ ranging from 30 to 35° in Fig. 2b shows that the diffraction peaks of Mn^{2+}-doped samples were located at a slightly higher angle than the undoped samples. This shift in XRD pattern can be attributed to the lattice contraction and indicates that the Mn^{2+} ions were dissolved in ZGO by replacing different ions and the lattice constant slightly changed with Mn^{2+} doping.

Given that the ionic radiation of Mn^{2+}, Zn^{2+}, and Ge^{4+} are 0.80, 0.74, and 0.53 Å, respectively [6], Mn^{2+} ions can replace Zn^{2+} ions in ZGO.

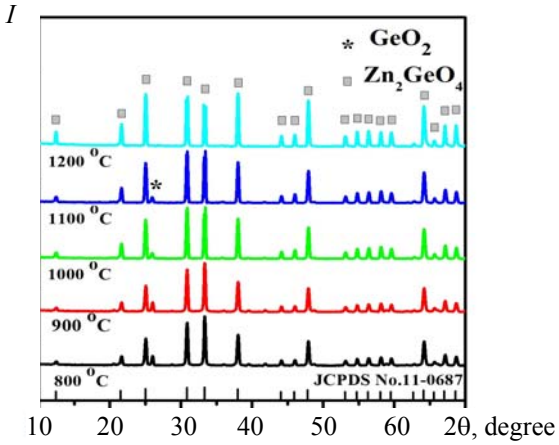

Fig. 1. XRD patterns of ZGO phosphor calcinated at different temperatures (800–1200°C) for 2 h.

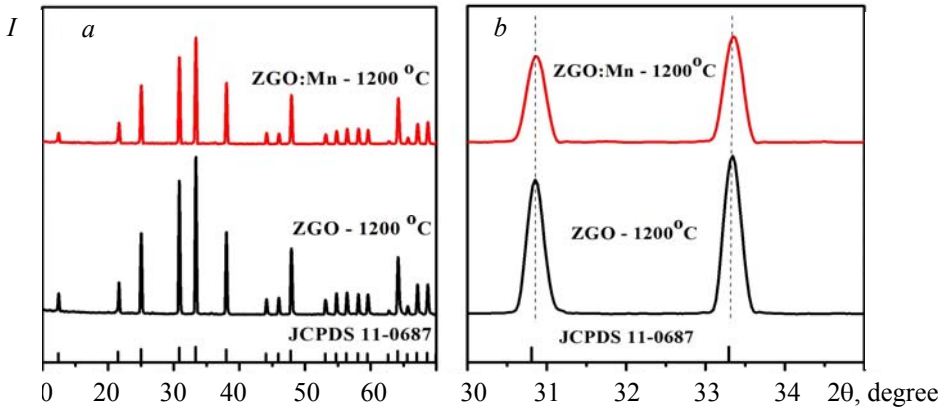

Fig. 2. (a) XRD patterns of ZGO and ZGO:0.05Mn^{2+} phosphors; (b) partially enlarged image of (113) and (410) peaks calcinated at 1200°C for 2 h.

Figure 3 shows the FESEM images of ZGO calcinated from 800 to 1200°C and ZGO:Mn^{2+} calcinated at 1200°C. All the ZGO samples and ZGO:0.05Mn^{2+} have granular and relatively uniform structure. As shown in Fig. 3a–e, the particle size of ZGO increased from several hundred nanometers (200–300 nm) to several micrometers (2–6 μm) with temperature (800–1200°C). No pure crystal ZGO can be formed at low temperatures, and an increase in temperature up to 1200°C can produce the best crystal quality of ZGO with a pure phase because the small particles agglomerate together to form particles up to several micrometers in diameter. The clear boundary between the particles proves that the prepared material has achieved good crystallization.

The properties of phosphor were investigated through UV-vis analysis to reveal the ability of Mn^{2+} ion to enter the ZGO lattice. Figure 4a shows that the optical absorbing margin of ZGO:Mn had slightly shifted to the energy region smaller than ZGO (4.68 eV). This band gap reduction is attributed to the electronic states associated with the Mn below the conduction band and further confirms the successful doping of Mn^{2+} ion into the ZGO host lattice. The results of EDS spectrum analysis in Fig. 4b, c also confirmed the presence of the three Zn, Ge, and O elements for the ZGO lattice and doped samples, apart from the three elements of the lattice. The addition of Mn elements is visible in Fig. 4c. No other elements, pure samples, and impurities were found. The percentage of elements corresponds to the formula of the material to be produced.

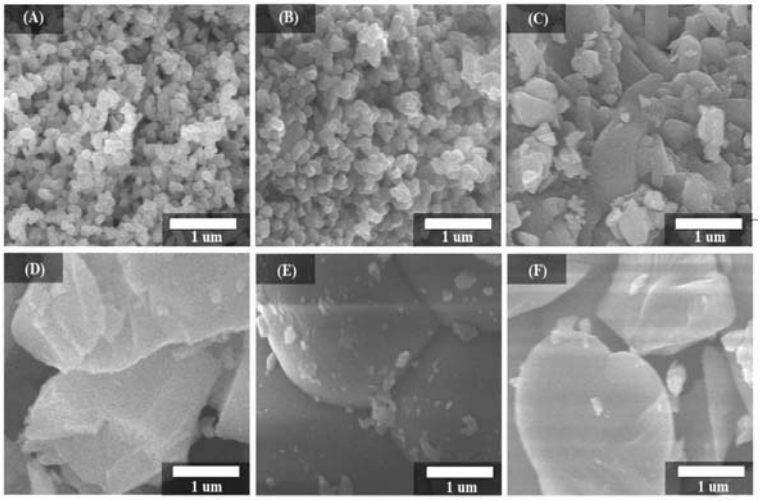

Fig. 3. FESEM of ZGO (a–e) calcinated from 800 to 1200°C and ZGO:0.05 Mn^{2+} (f) calcinated at 1200°C for 2 h.

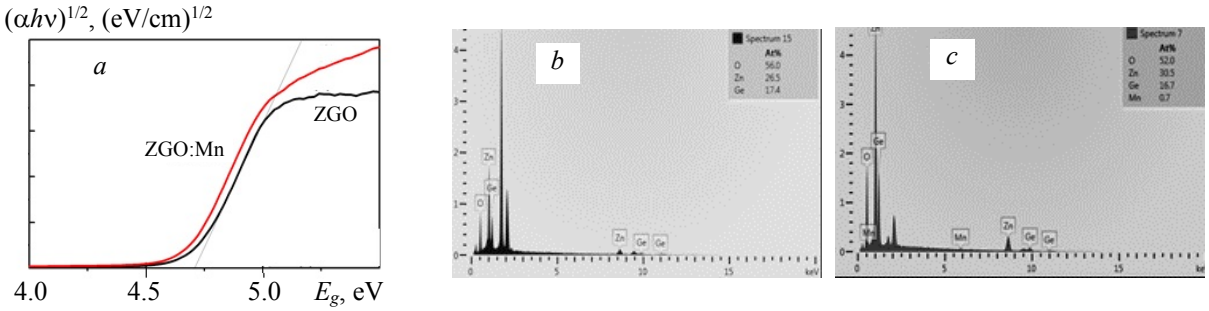

Fig. 4. (a) UV-vis and EDS (b, c) spectra of ZGO phosphors calcinated at 1200°C for 2 h.

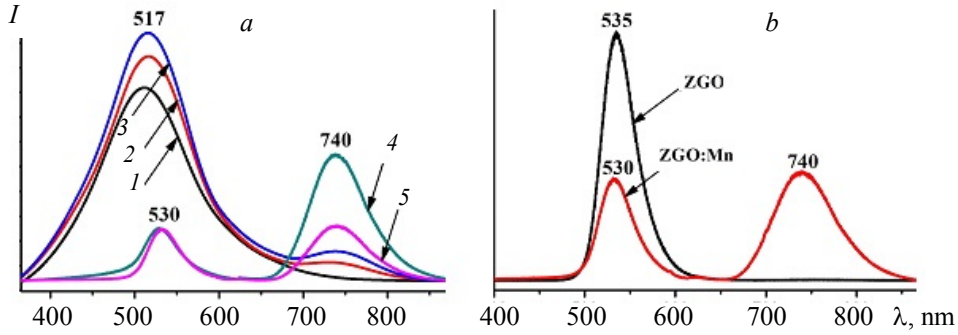

Fig. 5. (a) PL spectra of ZGO phosphors at different calcinated temperatures (800 (1), 900 (2), 1000 (3), 1100 (4), and 1200°C (5)); (b) PL spectra of ZGO and ZGO:Mn^{2+} phosphors calcinated at 1200°C for 2 h.

A UV light of 260 nm wavelength was used to excite ZGO and ZGO:Mn^{2+} calcinated at different temperatures and measure the photoluminescence (PL) spectra. Figure 5a presents the PL spectra of undoped ZGO samples calcinated at different temperatures. For the samples calcinated at temperatures lower than 1100°C, the PL spectra exhibited a strong broad band peaked at 517 nm and a weak near infrared (NIR) band centered at approximately 740 nm. When the calcinating temperature was increased from 800 to 1000°C, the intensity of both bands increased, and the NIR band became significant. For the samples calcinated at 1100 and 1200°C, two emission bands were found at 530 and 740 nm. The intensity ratio between these bands decreased when the calcinating temperature was increased from 1100 to 1200°C. For all the samples, the emissions located at 517 and 530 nm, which are different from those previously reported, can be attributed to

the native defect of ZGO [1]. The NIR band centered at approximately 740 nm can be attributed to defects such as oxygen vacancy (V_O), interstitial zinc (Zn_i), interstitial oxygen (O_i), and/or other reasons [7, 8]. For example, the NIR emission at 670–740 nm was assigned to V_O and Zn_i [9]. This finding suggests that the origin of NIR emission (approximately 740 nm) could be related to the transfer of energy from non-bridging oxygen-hole centers (NBOHs) to zinc (Zn_i) and oxygen-vacant state (V_O) in the ZGO host lattice. The peak intensity of NIR emission band at 740 nm increases gradually with the calcinating temperature, reaches the maximum value at 1100°C, and decreases with further increase in the calcinating temperature. This phenomenon occurd because at 800–1100°C calcination, the phase GeO_2 still remains in the samples and thus affects the intensity of 740 nm band. At high temperature of 1200°C, GeO_2 no longer exists in ZGO host lattice, and the intensity of the NIR band is reduced. As predicted, the melting temperature of GeO_2 at 1115°C is the main reason. This result is consistent with the X-ray images of the ZGO samples.

Figure 5b illustrates the typical PL emission spectrum of ZGO:Mn^{2+} calcinated at 1200°C. The PL spectrum of undoped ZGO calcinated at the same temperature is also presented for comparison. The emission spectrum of ZGO:Mn^{2+} shows only a green emission band centered at 535 nm with a full width at half maximum of approximately 42 nm. The NIR band observed in the PL spectrum of undoped ZGO disappeared completely. The green emission can be attributed to the parity-forbidden *d-d* transition from the lowest excited state $^4T_1(^4G)$ to the ground state $^6A_1(^6S)$ of Mn^{2+} ions [10, 11]. The luminescence of the Mn^{2+} ion depends on the ZGO host crystal field. The Mn^{2+} ions in the ZGO host with relatively high crystallinity experience a strong crystal field. Increasing the crystal field reduces the energy difference of the ground and first excited states, resulting in peak broadening and red-shift of the emission peak [12]. The emission at 535 nm corresponds to the *d-d* transition of Mn^{2+} through the energy transfer from ZGO [13, 14]. Each Mn^{2+} ion occupying a Zn^{2+} site is coordinated to four oxygen atoms. Thus, Mn^{2+} ions can either play an important role in the fluorescence quenching of the NIR band at wavelength of 740 nm or act as the main agents preventing energy conversion from NBOHs into the ZGO host lattice.

On the basis of the above results, the energy level diagram and the luminescence mechanism of the Mn^{2+}-doped and pure ZGO samples are illustrated in Fig. 6. During 260 nm excitation, the electrons and free holes are created through region transformation. Free electrons in the conduction band tend to be trapped by electron traps in the restricted zone through a non-radiating process. Electron traps are associated with interstitial zinc and oxygen vacancies, which are intrinsic defects in the ZGO host lattice and act as donor levels in the host lattice emission. Furthermore, the holes are trapped by cation gaps, which act as the acceptor [9]. Recombination of electrons in electron traps and holes in the valence band results in blue emission at the 517 nm region of the host lattice [15], energy transfer from NBOHs to Zn_i, and oxygen vacancy (Vo) states in the ZGO host lattice showing an emissivity peak at 740 nm. After Mn^{2+} ion doping into the ZGO host lattice, Mn^{2+} acts as the optical center and reduces the defects of the host lattice. Therefore, in the luminescent spectrum of ZGO:Mn^{2+} samples, the emissive peak appears only as the characteristic peak of Mn^{2+} at 535 nm. The electrons in the host lattice can also transfer their energies to the $^4T_2(G)$ level of Mn^{2+} and recover to the $^4T_1(G)$ level with the help of phonons, resulting in the green emission of Mn^{2+} from the transition of $^4T_1(G) \rightarrow {}^6A_1(S)$.

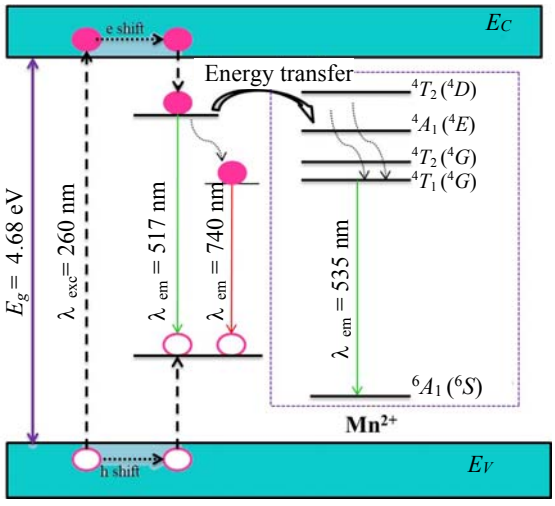

Fig. 6. Energy level diagram and scheme explaining their PL spectra and host to Mn energy transfer.

Conclusions. Pure and 5% Mn^{2+}-doped ZGO phosphors were successfully synthesized via co-precipitation and subsequent calcination at 1200°C. Systematic investigations were performed using XRD, photoluminescence spectroscopy, and FESEM-EDS. The effect of calcining temperature on the luminescent properties of undoped ZGO was studied. A clear explanation on the luminescent mechanism of ZGO material and the quenching of NIR band (~740 nm) of ZGO:Mn^{2+} was given. The white–bluish, green, and near infrared emission of ZGO host were attributed to the native defects and the transfer of energy from NBOHs into the ZGO host lattice. Under UV excitation, the Mn^{2+}-activated ZGO phosphors exhibit a strong green emission band, making it a promising, green-emitting luminescent material with potential applications in LEDs. The emission control of ZGO powders in the near infrared region opens up the possible utilization of phosphor for agriculture lighting.

Acknowledgments. This research is funded by the Hanoi University of Science and Technology (HUST) under project number T2018-PC-202

REFERENCES

1. Z. Liu, X. Jing, L. Wang, *J. Electrochem. Soc*., **154**, H500 (2007).
2. Liang Zhao, Shuang Yao, Huayin Sun, Qian Huang, Tao Wen, Jing Du, *J. Mater. Sci.: Mater. Electron*., https://doi.org/10.1007/s10854-018-0440-z
3. Pedro Hidalgo, Alejandro López, Bianchi Méndez, Javier Piqueras, *Synthesis and Optical Properties of Zn_2GeO_4 Microrods*, **104**, 84–90, 1 February (2016).
4. Satoru Takeshita, Joji Honda, Tetsuhiko Isobe, Tomohiro Sawayama, Seiji Niikura, *Cryst. Growth Des.*, **10**, No. 10 (2010).
5. Qiuhong Zhang, Jing Wang, *Appl. Phys. A*, **108**, 943–948 (2012).
6. Yan Cong, Yangyang He, Bin Dong, Yu Xiao, Limei Wang, *Opt. Mater.* (**2015**), http://dx.doi.org/10.1016/j.optmat.2015.01.045.
7. A. Janotti, C. G. Van de Walle, *Phys. Rev. B*, **76** (2007) 165202.
8. X. Xu, C. Xu, J. Dai, J. Pan, J. Hu, *J. Phys. Chem. Solids*, **73**, 858–862 (2012).
9. G. J. Gao, L. Wondraczek, *J. Mater. Chem. C*, **1**, 1952–1958 (2013).
10. H. He, Y. Zhang, Q. Pan, G. Wu, G. Dong, J. Qiu, *J. Mater. Chem*., **C3**, 5419–5429 (2015).
11. R. Selomulya, S. Ski, K. Pita, C. H. Kam, Q. Y. Zhang, S. Buddhudu, *J. Mater. Sci. Eng*., **B 100**, 136–141 (2003).
12. P. Thiyagarajan, M. Kottaisamy, M. S. Ramachandra Rao, *Scr. Mater*., **57**, 433–436 (2007).
13. X. Li, F. Chen, *Mater. Res. Bull*., **48**, 2304–2307 (2013).
14. N. Taghavinia, G. Lerondela, H. Makino, A. Yamamoto, T. Yao, Y. Kawazoe, T. Goto, *J. Nanotechnol*., **12**, 547–551 (2001).
15. T. Cu, *J. Phys. Soc. Jpn.*, **75**, 1–5 (2006).